Author(s): Jelovica, Jasmin & Romanoff, Jani & Remes, Heikki

Title: Influence of general corrosion on buckling strength of laser-welded web-core sandwich plates

Year: 2014

Version: Post print

Please cite the original version:

Jelovica, Jasmin & Romanoff, Jani & Remes, Heikki. 2014. Influence of general corrosion on buckling strength of laser-welded web-core sandwich plates. Journal of Constructional Steel Research. Volume 101. p. 342-350. DOI: 10.1016/j.jcsr.2014.05.025.

Jelovica, J., Romanoff, J. and Remes, H. "Influence of general corrosion on buckling strength of laser-welded web-core sandwich plates", Journal of Constructional Steel Research, Vol.101, 2014, p. 342-350.

Influence of general corrosion on buckling strength of laser-welded web-core sandwich plates

J. Jelovica[1], J. Romanoff, H. Remes

Department of Applied Mechanics/Marine Technology, Aalto University School of Engineering, P.O. Box 15300, 00076 Aalto, Finland

Abstract

The strength of a web-core steel sandwich plate is potentially reduced in a corrosive environment. This study is dedicated to the influence of a reduction in the thickness of the plates as a result of general corrosion on sandwich plate buckling strength and first-fibre failure. Two scenarios are investigated in which corrosion reduces the thickness of (a) the outer sides of the face plates and (b) all surfaces, including the core. The laser weld between the face sheets and the core is assumed to be intact. The assumptions are made on the basis of earlier experimental findings. Critical buckling and geometric non-linear analysis are carried out with the finite element method, with the kinematics being represented using two approaches: (1) equivalent single-layer with first-order shear deformation theory, and (2) a three-dimensional model of the actual geometry of the structure, modelled using shell and connector elements. The former is used to identify the effect of corrosion on the stiffness coefficients and, consequently, the buckling strength. The later is used for verification and for stress prediction during post-buckling. A rapid decrease in the buckling strength was found for corrosion affecting the outer sides of the sandwich plate. The decrease in the buckling strength doubled in the case of the diffusion of moisture (water) into the core. The shear-induced secondary bending of the faces was found to affect the first-fibre yield.

Keywords: web-core sandwich plate; buckling; post-buckling; corrosion; first-fibre failure; laser-weld.

List of symbols

a	Length of the sandwich plate (m)
b	Width of the sandwich plate (m)
d	Distance between neutral axes of the face-plates (mm)
t_f	Thickness of the face-plate (m)
t_w	Thickness of the web-plate (mm)
s	Spacing of the web-plates (mm)
h_c	Height of the sandwich plate core (mm)
m	Number of buckling half-waves in x-direction

[1] Corresponding author. Tel: +358 50 4088 957. E-mail: jasmin.jelovica@aalto.fi

n	Number of buckling half-waves in y-direction
k_θ	Rotational stiffness of the T-joint (kN)
u	Displacement component in x-direction (m)
v	Displacement component in y-direction (m)
w	Deflection of the plate (m)
A_{ij}	Extensional stiffness of the sandwich plate, i,j = 1,2,3. (N/m)
B_{ij}	Bending-extensional coupling stiffness of the sandwich plate, i,j = 1,2,3. (N)
D_{ij}	Bending stiffness of the sandwich plate, i,j = 1,2,3. (Nm)
D_{f}	Bending stiffness of the face-plate (Nm)
D_{Qx}	Transverse shear stiffness in x-direction (Nm)
D_{Qy}	Transverse shear stiffness in y-direction (Nm)
D_{w}	Bending stiffness of the web-plate (Nm)
E	Young's modulus (Pa)
G	Shear modulus (Pa)
M	Moment acting on the T-joint (Nm)
N_0	Buckling load per unit width (N)
ν	Poisson's ratio
θ_x	Rotation around y-axis
θ_y	Rotation around x-axis
θ_c	Deviation from the 90° angle at the T-joint

1 Introduction

All-steel web-core sandwich plates are made from unidirectional web plates in the core, welded to the face plates by laser welding; see Fig. 1. The discrete nature of the structure in the transverse direction makes the sandwich plate highly orthotropic, with a severe discrepancy between the transverse shear stiffness in the x- and y-directions. The choice of steel as a material makes these structures convenient to incorporate into large assemblies such as bridges, ships, and offshore structures, while still offering weight reductions in comparison to traditional structures. However, such applications expose the sandwich plate to a corrosive environment as a result of the presence of sea water. Corrosion is known to lead to a reduction in the thickness of structural members and degradation of their mechanical properties (see e.g. Rahgozar [1], Saad-Eldeen et al. [2]). A sandwich plate typically features thin plates and several surfaces exposed to corrosion if water enters the core. Therefore, the influence of corrosion on their strength is an important practical issue.

The influence of corrosion on sandwich beams has been investigated in the European Union Sandwich project [3] and the investigation of DNV [4]. However, these experiments were focused on observing corrosion wastage rates and the influence on stiffness only in the linear elastic regime. Jelovica et al. [5] presented ultimate strength experiments on sandwich beams in three-point bending. The specimens had previously been submerged in water for up to two years. It was observed that the plates were primarily affected by general corrosion. The corrosion rates were measured. Furthermore, numerical simulations with a three-dimensional (3D) structure based on the average plate thickness and neglect of the residual stresses showed good agreement with the experimental results. It was furthermore found that corrosion had negligible effect on the welds from those same specimens; see Aromaa et al. [6]. The present study is motivated by the gap in the literature related to the influence of corrosion on the behaviour of the sandwich plate under compression. The review of corrosion studies given below provides a background for the present work.

Several types of corrosion exist, including general corrosion, pitting, grooving, crevice, etc. The most prevalent form of corrosion is a general loss of surface material; this condition results in a gradual thinning of the structure. In this study, general corrosion is considered, since the results from Refs. [4-6] indicate that the sandwich plate is affected by this type of corrosion in the most severe conditions, for a limited amount of time. Furthermore, in anticipation of corrosion, ship structural design according to the Common Structural Rules (DNV [7], DNV [8]) requires a uniform thickness allowance for structural members, depending on their location in a ship. There are studies which showdifferent corrosion rates in different parts of a ship, depending on the operational parameters of bulk carriers (see e.g. Gardiner and Melchers [9]) and tankers (see e.g. Tanker Structure Cooperative Forum [10]). The DNV guidelines for laser-welded sandwich panels [11] instruct corrosion protection to be performed in the same way as in the case of a stiffened plate structure. Although the corrosion rates for two structures might be the same under the same conditions, the reduction of the strength might be different as a result of the topology of the cross-section.

Web-core sandwich plates under compression were investigated in several studies without the influence of corrosion. Kolsters and Zenkert [12], Kolsters and Zenkert [13], and Kolsters [14] studied the local buckling and post-buckling behaviour of face plates. Taczala and Banasiak [15] presented the difference in critical buckling modes and stresses between sandwich and stiffened plates. Kozak [16] presented experiments on the ultimate strength of sandwich columns. Jelovica and Romanoff [17] studied the buckling and post-buckling behaviour of web-core sandwich plates where the rotational stiffness of the T-joint was assumed to be infinite. However, for laser-welded sandwich plates the stiffness of the T-joint has a finite value (Romanoff et al. [18]). Jelovica et al. [19] showed that the stiffness of the T-joint has a significant influence on the buckling strength of the sandwich plates. Thus, in analysis of the sandwich plate under a compressive load the stiffness of the joint must be considered in order to obtain a realistic post-buckling response. Furthermore, on the basis of Ref. [18] it can be expected that significant rotations at the joint will cause an increase in the stiffness as a result of the contact between the web and the face plate during the post-buckling regime. Therefore, this effect must be considered in the analysis.

This paper presents the influence of thickness reduction due to general corrosion on the buckling strength of laser-welded web-core sandwich plates. Additionally, stresses at first-fibre failure are studied. The results are viewed through plate thickness reduction instead of exposure time since the corrosion rates depend on the environmental conditions next to the structure. The corrosion is assumed to affect the sandwich plates by reducing the thickness of (a) the face plates from outside the sandwich plate or (b) all the plates, assuming that the water is present in the core as well. The weld is considered not to be affected by corrosion in this study, as is also shown in Refs. [4, 6]. Critical buckling and geometric non-linear analysis are carried out with the finite element method (FEM), with the kinematics being represented using two approaches: (1) equivalent single-layer (ESL) with first-order shear deformation theory (FSDT) and (2) a 3D model of the actual geometry of the structure, modelled using shell and connector elements. The corrosion is modelled by changing the plate stiffness coefficients for ESL and reducing the thickness of the plates in the 3D model. The rotational stiffness of the T-joint is taken as being constant, according to the available experimental data. The effect of the non-linear rotational stiffness caused by the contact between the plates beyond the experimental range is also studied with FEM. The plate dimensions are such that the structure suits the frame system of a ship, and global buckling is a dominant mode. The sandwich plate is loaded in the stiffener direction and the edges are simply supported. The loaded edges are straight, while the unloaded edges move in the plane of the plate. Linear elastic material behaviour is assumed.

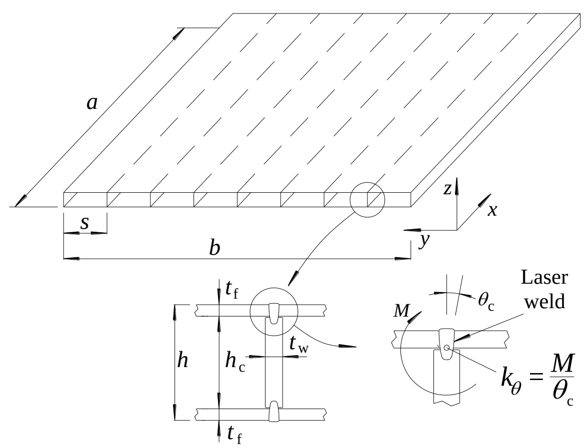

Fig. 1. *A laser-welded web-core sandwich plate.*

2 Effect of corrosion on the cross-section

On the basis of the experimental observations in Refs. [4-6], it is assumed that corrosion causes a uniform reduction in the thickness of the plates and has a negligible effect on the laser weld, i.e. pitting or crevice corrosion does not occur. Thickness reduction occurs in two ways: (1) outside the sandwich plate structure (Fig. 2a) and (2) both outside and inside the sandwich plate structure simultaneously (Fig. 2b). In the former case, the corrosion reduces the thickness of the face plate t_f on the outer side by the amount $t_{c,out}$, while the thickness of the web plate t_w and height of the core h_c remain the same. In the latter case, the corrosion reduces the thickness of the face plate by $t_{c,in\&out}$ on both sides, causing a reduction in the thickness of the face plate that is twice as high as in the previous case. The thickness of the web plate is also reduced by $t_{c,in\&out}$ on both sides. The corrosion in the core increases the height h_c by $2t_{c,in\&out}$. The weld is considered intact.

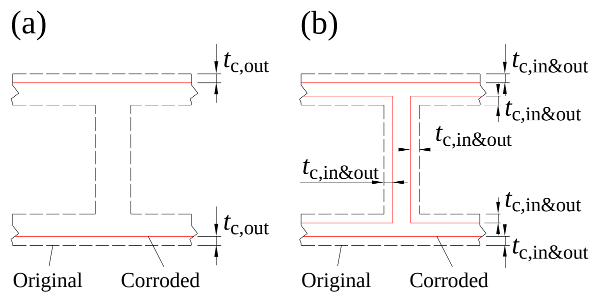

Fig. 2. *Cases of corrosion in the sandwich plate that were considered: a) outside; b) both inside and outside the structure.*

3 Analysis methods

Critical buckling and geometric non-linear analysis are carried out with FEM using the two aforementioned approaches, namely the ESL approach and the 3D model. The ESL results are directly affected by the reduction in the plate stiffness coefficients, while the 3D model gives more accurate deformations and stresses because it uses the actual geometry of the corroded structure. Analysis of the T-joint is performed separately beforehand to determine the rotational stiffness and the information used in the 3D analysis.

Geometric non-linear analysis is carried out by increasing the compressive load on the initial imperfect structure in small steps. The first eigenmode is used as the shape of the initial imperfection and is given the magnitude of 0.01% of the plate length. The analysis is carried out using the Abaqus software, version 6.9, with the modified Riks procedure to trace the post-equilibrium path (see Abaqus [20]). A subspace iteration solver is used for the eigenvalue analysis. The modelling aspects of the two approaches are discussed in the next two sections.

3.1 ESL approach with FSDT

The sandwich plate is modelled as an orthotropic plate, which is analyzed as an equivalent single-layer with the first-order shear deformation plate theory. The plate extensional, bending-extensional coupling, bending, and shear stiffnesses are defined through [A], [B], [D], and [D_Q] matrices, respectively. A symmetric web-core sandwich plate is a special type of orthotropic plate where the stiffness coefficients A_{13}, A_{23}, D_{13}, D_{23}, and B_{ij} are equal to zero. The extension stiffnesses for the orthotropic plate at hand can be expressed as

$$A_{11} = 2E't_{\mathrm{f}} + \frac{Eh_{\mathrm{c}}}{s}t_{\mathrm{w}};$$
$$A_{12} = 2\nu E't_{\mathrm{f}};$$
$$A_{22} = 2E't_{\mathrm{f}};$$
$$A_{33} = 2Gt_{\mathrm{f}};$$ (0)

where $E' = E\big/\left(1-\nu^2\right)$. It can be seen that the extension stiffnesses depend linearly on the thicknesses of the face plate and web plate.

The bending stiffnesses are given by

$$D_{11} = \frac{h_{\mathrm{c}}^3}{12}\left[2E'\left\{3\cdot\frac{t_{\mathrm{f}}}{h_{\mathrm{c}}} + 6\cdot\left(\frac{t_{\mathrm{f}}}{h_{\mathrm{c}}}\right)^2 + 4\cdot\left(\frac{t_{\mathrm{f}}}{h_{\mathrm{c}}}\right)^3\right\} + E\frac{t_{\mathrm{w}}}{s}\right],$$
$$D_{12} = \frac{h_{\mathrm{c}}^3}{12}\left[2\nu E'\left\{3\cdot\frac{t_{\mathrm{f}}}{h_{\mathrm{c}}} + 6\cdot\left(\frac{t_{\mathrm{f}}}{h_{\mathrm{c}}}\right)^2 + 4\cdot\left(\frac{t_{\mathrm{f}}}{h_{\mathrm{c}}}\right)^3\right\}\right],$$
$$D_{22} = \frac{h_{\mathrm{c}}^3}{12}\left[2E'\left\{3\cdot\frac{t_{\mathrm{f}}}{h_{\mathrm{c}}} + 6\cdot\left(\frac{t_{\mathrm{f}}}{h_{\mathrm{c}}}\right)^2 + 4\cdot\left(\frac{t_{\mathrm{f}}}{h_{\mathrm{c}}}\right)^3\right\}\right],$$
$$D_{33} = \frac{h_{\mathrm{c}}^3}{12}\left[2G\left\{3\cdot\frac{t_{\mathrm{f}}}{h_{\mathrm{c}}} + 6\cdot\left(\frac{t_{\mathrm{f}}}{h_{\mathrm{c}}}\right)^2 + 4\cdot\left(\frac{t_{\mathrm{f}}}{h_{\mathrm{c}}}\right)^3\right\}\right].$$ (0)

Since, typically, $t_{\mathrm{f}} << h_{\mathrm{c}}$, the higher-order (square and cubic) terms of the ratio (t_{f} / h_{c}) are negligible and thus have an insignificant influence on the bending stiffness coefficients, which then depend linearly on the thicknesses of the face and web plates for a constant core height h_{c}.

The transverse shear stiffness in the web plate direction for a symmetric plate [21] is equal to

$$D_{Q\mathrm{x}} = k_{11}^2\left(2G_{\mathrm{f}}t_{\mathrm{f}} + \frac{t_{\mathrm{w}}}{s}Gh_{\mathrm{c}}\right),$$ (0)

where

$$k_{11} = \sqrt{\frac{1}{A\left(\sum_i \int \left(\frac{\tau_i}{Q_{Q\mathrm{x}}s}\right)^2 t_i \mathrm{d}s_i\right)}}, \quad i = \mathrm{t,c,b}.$$ (0)

The transverse shear stiffness in the opposite direction to the web plate direction is [21] (for a symmetric plate)

$$D_{Qy} = \frac{12D_w}{s^2\left(k_Q\left(\frac{D_w}{D_f}+6\frac{d}{s}\right)+12\frac{D_w}{k_\theta \cdot s}-2\frac{d}{s}\right)} \quad (0)$$

where

$$k_Q = \frac{1+6\frac{D_f}{D_w}\frac{d}{s}}{2+12\frac{D_f}{D_w}\frac{d}{s}}, \quad (0)$$

The T-joint rotational stiffness is defined as the ratio of the moment M to the rotation angle θ_c at the weld (see Fig. 1):

$$k_\theta = \frac{M}{\theta_c}, \quad (0)$$

3.1.1 Analytical solution for buckling

The exact buckling load per unit width of the sandwich plate with simply supported edges is given by Reddy [22] and Robinson [23]. The expression is presented in closed form as

$$N_0 = \frac{c_{33}+\left(\frac{\alpha^2}{D_{Qy}}+\frac{\beta^2}{D_{Qx}}\right)\cdot c_1}{\alpha^2\cdot\left(1+\frac{c_1}{D_{Qx}\cdot D_{Qy}}+\frac{c_2}{D_{Qx}}+\frac{c_3}{D_{Qy}}\right)}. \quad (0)$$

where

$\alpha = m\cdot\pi/a$;

$\beta = n\cdot\pi/b$;

$c_{33} = D_{11}\cdot\alpha^4 + 2\left(D_{12}+2D_{33}\right)\alpha^2\beta^2 + D_{22}\beta^4$;

$c_1 = c_2\cdot c_3 - \left(c_4\right)^2$;

$c_2 = D_{11}\cdot\alpha^2 + D_{33}\cdot\beta^2$;

$c_3 = D_{33}\cdot\alpha^2 + D_{22}\cdot\beta^2$;

$c_4 = \left(D_{12}+D_{33}\right)\cdot\alpha\cdot\beta.$

Multiplication of the buckling load in Eq. (0) by the plate width b and minimization with respect to m and n gives the buckling strength (i.e. the minimum buckling load) of the plate.

3.1.2 2D model

The geometric non-linear (i.e. post-buckling) analysis is carried out using the FEM program (Abaqus). Equivalent stiffness properties are assigned to a single layer in the geometrical mid-plane of the structure, where the loads and boundary conditions are also defined. Shell elements with four nodes (S4) are used. The mesh consists of 100 elements in the length direction and 100 elements in the width direction. The transverse deflection is zero at the edges and no rotation is allowed about the axis perpendicular to the edge on the loaded sides; that is, the edges are required to stay straight. The typical deformed shape of the plate is shown in Fig. 3.

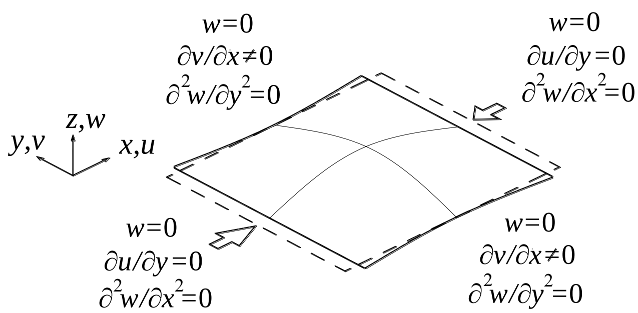

Fig. 3. *Simply supported plate with unloaded edges free to move in-plane. The dashed lines show the unloaded plate and the solid lines show the (exaggerated) post-buckled shape (2D model).*

3.2 3D model

The 3D geometry of the structure is modelled using shell elements (S4). Connector-type elements (CONN3D2) are used to connect the web and face plate at their intersection. The moment-angle relationship for the connector elements is defined from experimental results [18] or from the analysis described in the Appendix for higher rotation angles. Concentrated nodal forces act at the nodes in the neutral axis. Six shell elements per web plate height are used. The face plates have six shell elements between the webs.

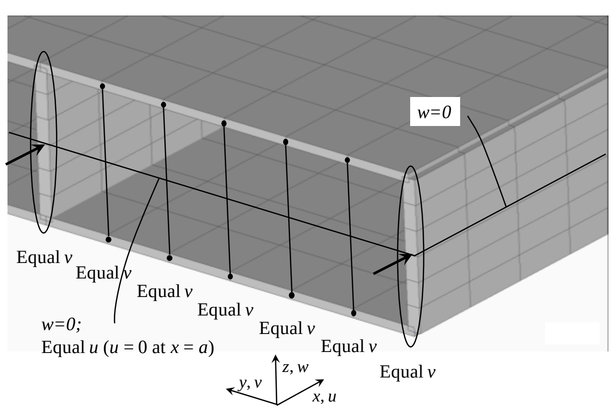

Fig. 4. *The FE mesh and the boundary conditions for the 3D model of the sandwich plate.*

Simply supported boundary conditions are considered, with the loaded edges kept straight and the unloaded edges free to move in-plane. The transverse deflection is zero only at the nodes at the geometric mid-plane. This allows the rotation of the plate around the mid-plane edge. Furthermore, all the nodes of a certain web plate have the same displacement v in the y-direction; see Fig. 4. Additionally, the nodes at the geometric mid-plane at $x = 0$ are required to have the same displacement u in the x-direction. The same is required at $x = a$.

4 Analysis and results

The sandwich plate that is studied is a standard web-core sandwich plate for marine and civil applications. It features the following values for the thickness of the face plates t_f, the web plate thickness t_w, the height of the core h_c, and the spacing of the web plates s:

$$t_f = 2.5\,\text{mm},\ t_w = 4\,\text{mm},\ h_c = 40\,\text{mm},\ s = 120\,\text{mm}.$$

The rotational stiffness of the T-joint is taken as being 107 kNm/m [18], while the effect of joint nonlinearity is presented in Section 4.4. The size of the plate is 3.6 m × 3.6 m. The material behaviour is assumed to be linear elastic, characterized by a Young's modulus E = 206 GPa and a Poisson's ratio $\nu = 0.3$.

Jelovica et al. [5] measured corrosion rates for this type of sandwich plate for an exposure time of a maximum of two years. In their work both cases of outer corrosion only or both inner and outer corrosion were observed. The thickness reduction rate was, on average, 0.1 mm/year per exposed surface. This was found to be in line with the measurements by Melchers et al. [24] for immersed plates.

For analysis using ESL, the stiffness coefficients are calculated on the basis of Eq. (0) and Eq. (0) . For 3D analysis, the thickness is modified directly.

4.1 Influence of general corrosion on stiffness coefficients and buckling strength

Fig. 5(a)-(c) shows that the reduction in the extensional and bending stiffness is linear for the web-core sandwich plate, while the nonlinearity of the transverse shear stiffness is negligible. Furthermore, it can be seen that the corrosion of the core causes a rate of reduction of stiffness that is twice as high as only corrosion outside the structure. In this case, both surfaces of the face plate are exposed to corrosion and thus the total reduction of the thickness is double that of the single side.

Fig. 5(d) presents the decrease in the buckling strength resulting from the reduction of the thickness; a linear decrease in the strength is observed. For a decrease in the thickness of 0.5 mm, the reduction of the buckling strength is 25.5% in the case of outer corrosion and 51% in the case of inner and outer corrosion. Thus the rate is two times higher when the core corrodes as well. If the reduction of the thickness is doubled to 1.0 mm, the reduction of the buckling strength also doubles. The linear relation between the buckling strength and the thickness of the plate is caused by the linear influence of the thickness on the bending and shear stiffness coefficients.

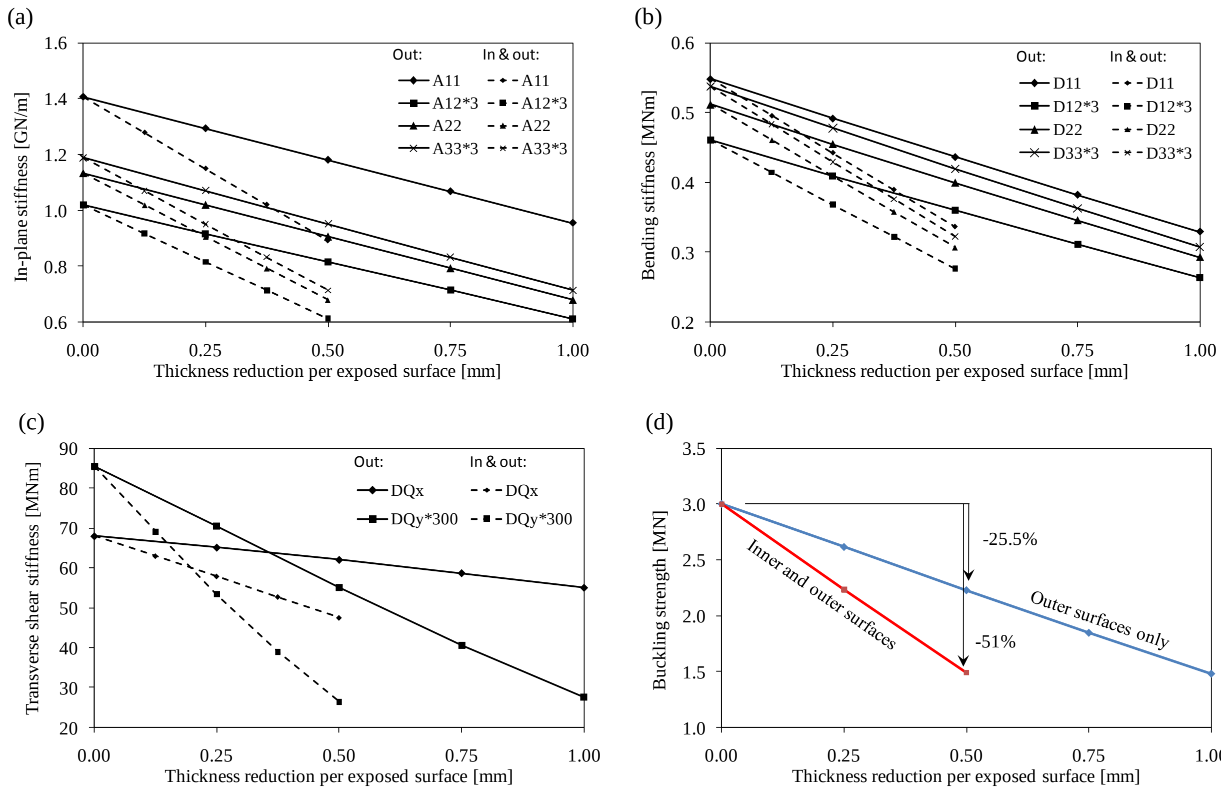

Fig. 5. *Influence of corrosion on the stiffness coefficients of the sandwich plate: (a) extensional, (b) bending, (c) transverse shear, and (d) buckling strength.*

4.2 Influence of general corrosion on non-linear behaviour

The load-shortening curves of the sandwich plate with the corrosion of the outer surfaces are presented in Fig. 6(a). The results with both the 2D and 3D models are presented, showing excellent agreement between the two. The buckling strength agrees closely with the analytical values, being regularly about 2% higher for the 3D solution. The 3D solution is presented until the first-fibre failure, defined here as the point where the von Mises stress at any point in the sandwich plate reaches 355 MPa. The load-deflection curves of the same corrosion case with the 3D model are shown in Fig. 6(b). Beside the reduction of the buckling strength, the corrosion also reduces the pre- and post-buckling stiffness of the plate. The load at which the first-fibre yielding occurs is reduced in the same rate, i.e. 25% for 0.5 mm thickness reduction and 49% for 1.0 mm thickness reduction. The devastating effect of the corrosion of all the surfaces is seen in the load-shortening curves in Fig. 6(c) in comparison with the same reduction of the thickness but outside the sandwich plate.

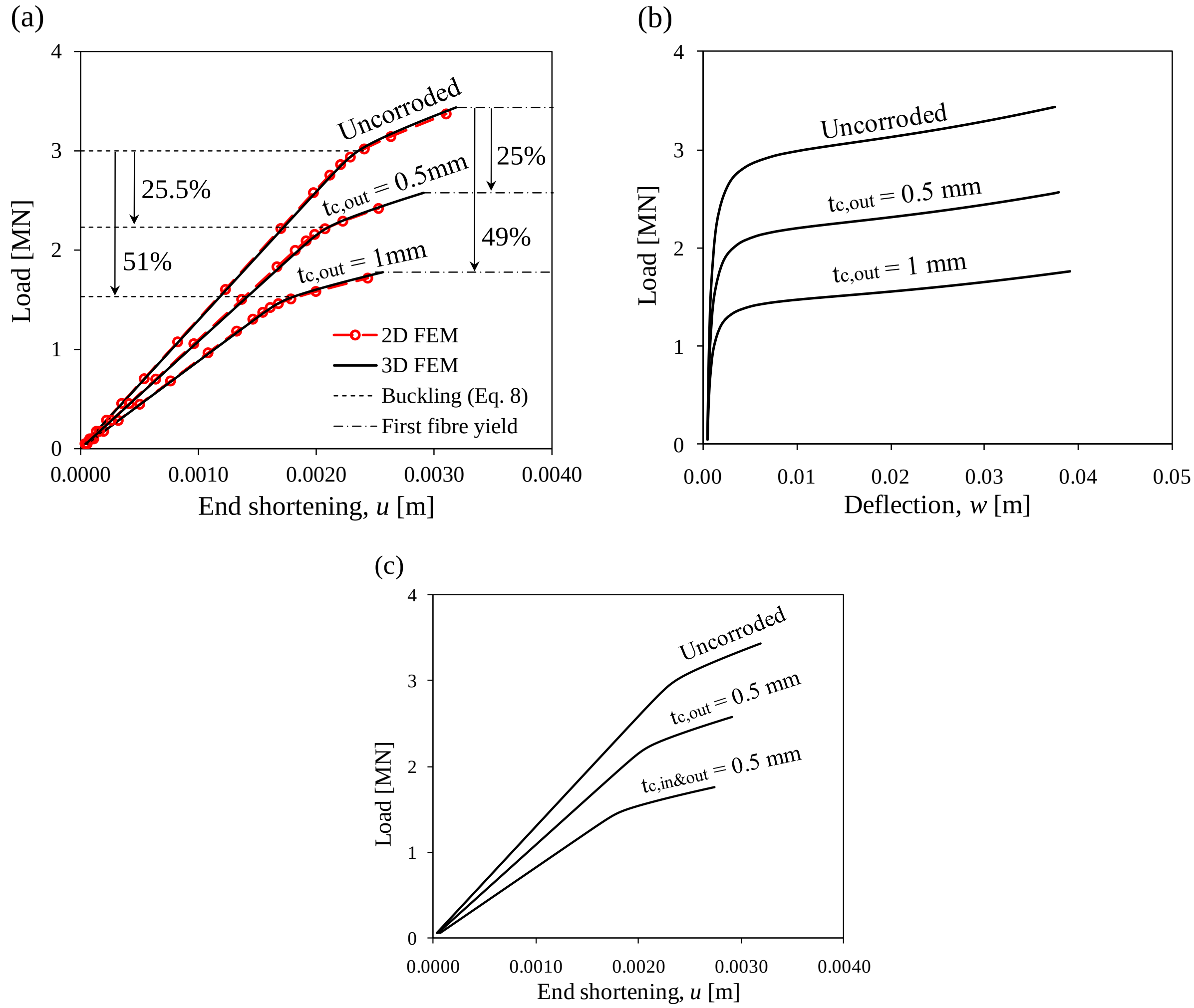

Fig. 6. *(a) Load-shortening and (b) load-deflection curves of sandwich plate with outer corrosion; (c) comparison of load-shortening for the two corrosion cases that were studied.*

4.3 Influence of general corrosion on first-fibre failure

The stress of 355 MPa is reached in the sandwich plate with a 1-mm reduction of its thickness caused by outer corrosion at smaller in-plane displacement and higher deflection than the uncorroded plate, as expected. The higher deflections of the corroded plate (Fig. 7a) are the result of its reduced ability to carry transverse shear forces (Fig. 7b). In both structures, the maximum normal stresses occur at $x = a/2$. That is where the shear force in the y-direction is at its highest, which results in high local bending stresses σ_y in the face plates. Fig. 8(a) and Fig. 8(b) present the normal stresses in the x- and y-directions, respectively, for the outer surface of the face plate on the concave side at $x = a/2$. The stresses are highest next to the unloaded edge ($y = 0$, b). Thus, the material yielding occurs at $x = a/2$, $y = 0$ and $x = a/2$, $y = b$; see Fig. 8(c). However, the ratio between σ_x and σ_y is not the same for two plates. Although σ_x is lower in the plate with thinner faces (-37%), σ_y is higher (+14%) as a result of greater local bending. The von Mises stress is significantly influenced by normal stress in the y-direction and, therefore, consideration of secondary stresses is important for failure assessment. This can also be seen from the membrane stress in the *x*-direction, which is significantly lower than 355 MPa (Fig. 8d). If the first-fibre yield would be assessed based on membrane stress only, the 355 MPa would be reached at 4.05 MN (+15%) for uncorroded plate.

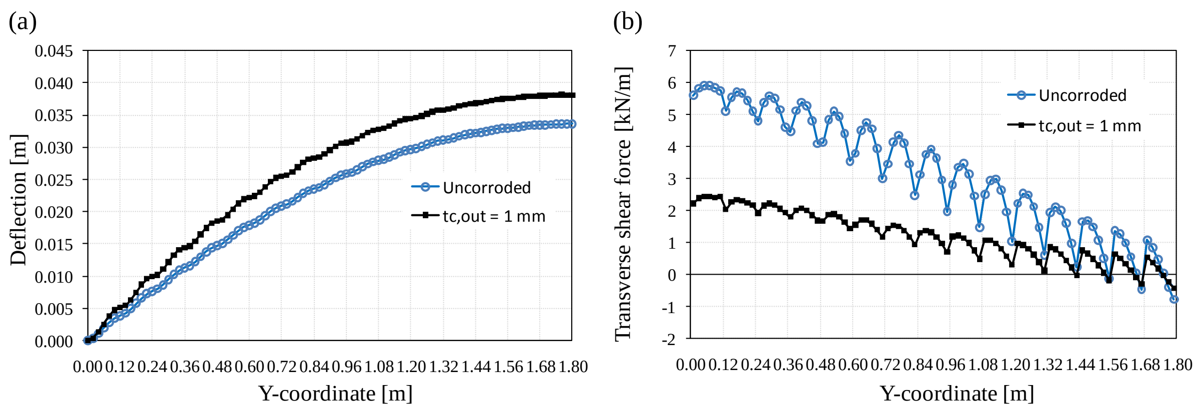

Fig. 7. *Comparison of (a) deflections* w *and (b) transverse shear force* Q_y *of the face plate on the concave side at* x = a/2.

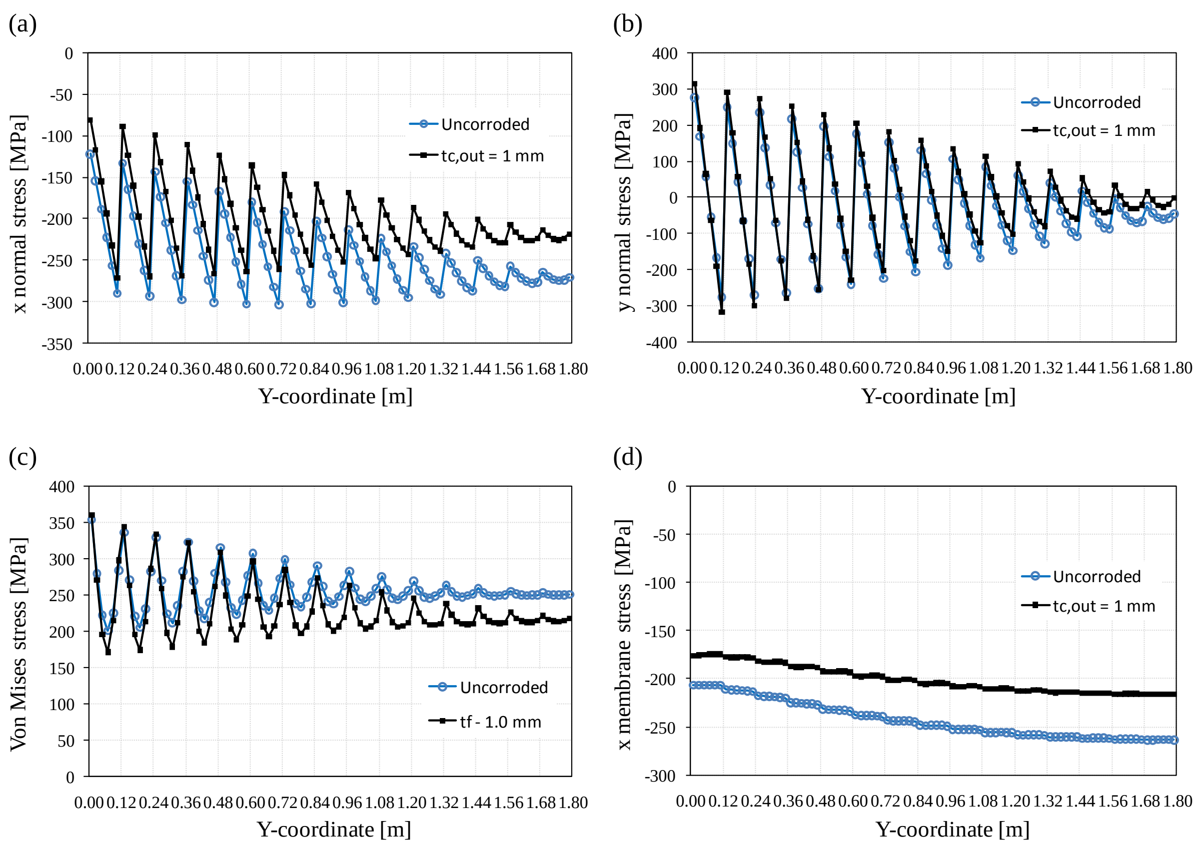

Fig. 8. *Comparison of (a) normal stress in the* x*-direction* σ_x*, (b) normal stress in the* y*-direction* σ_y*, (c) von Mises stress, and (d) membrane stress* σ_x *for the outer surface of the face plate on the concave side at* x = a/2.

4.4 Influence of T-joint stiffness on post-buckling response

Rotation in the T-joint after the contact between the face and the web plate increases the rotational stiffness, as shown in the Appendix. The rotation angle at which it happens is controlled by the root gap h_{rg} at the joint. The increase in the stiffness of the joint results in an increase in the transverse shear stiffness in the *y*-direction; see Eq. (0). The effect of this on the post-buckling response of the sandwich plate is shown in Fig. 9. It can be seen that the contact in the joint increases the load-carrying capability of the plate, but the influence is not significant. The smaller root gap results in a higher load-carrying capacity. The effect is reduced in the corroded plate because of the thinner plates. Ultimate moment in the joint is not reached in any case. The response of the sandwich plate with infinite joint stiffness is shown for comparison. It corresponds to the case of the thickness of the laser weld being equal to the thickness of the web plate. Infinite joint stiffness increases the buckling strength, but this effect decreases in the case of corroded plates.

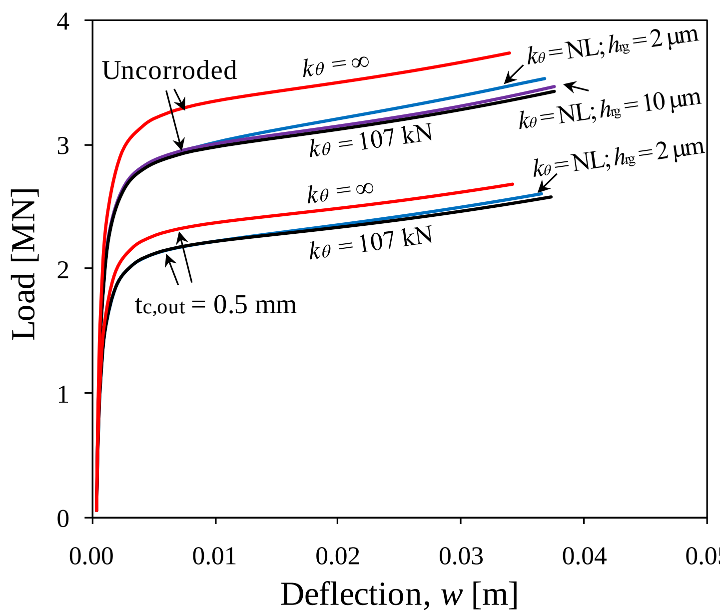

Fig. 9. *Influence of T-joint stiffness on the response of the sandwich plate.*

5 Discussion and conclusion

The study focused on the influence of plate thickness reduction due to general corrosion on the buckling strength and first-fibre failure of laser-welded web-core sandwich plates. The corrosion scenario is based on experimental observations [4-6]. The structure is affected by general corrosion from (a) outside and (b) both inside and outside the sandwich plate. In both cases, the degradation of the stiffness and the buckling strength is found to depend linearly on the reduction of the thickness. The decrease in the buckling strength for a reduction of 0.5 mm in the thickness of the face plates is 25.5%, which is quite severe. The load at first-fibre yield is reduced by 25%, which means that the safety margin between the design point of the structure and the onset of material failure remains unaffected. Furthermore, this study found that the reduction of the buckling strength doubles if the corrosion affects the core of the sandwich plate in addition to the outer side of the faces. Therefore, general corrosion needs to be avoided in web-core sandwich plates. It can be concluded that the benefits of a sandwich plate in terms of high bending stiffness and strength can become its weakness when corrosion takes place.

The corrosion of a sandwich plate reduces its ability to carry a transverse shear force, which increases shear deformation and, and hence, plate deflections during the post-buckling. Increased shear deformation of unit cells increases secondary bending in the transverse direction and, therefore, the shear-induced normal stress, as was shown by Romanoff and Varsta [25]. Thus the ratio of the von Mises stress components changes, increasing the share of σ_y for a corroded plate. It is furthermore shown that membrane stress is insufficient for the assessment of first-fibre failure, and local bending stress resulting from the periodic nature of the structure needs to be considered, especially for corroded plates. This contradicts the work of Kolsters and Wennhage [26], where first-fibre failure was assessed using membrane stresses only. Omitting the shear-induced normal stress overestimates the first-fibre yield load by 15% in uncorroded sandwich plate. This can also be the reason for the difference between the analytical and experimental failure load of a corrugated sandwich plate (also called a corrugated board) in Nordstrand [27]. The analytical approach did not consider the secondary bending. The experimental failure load was 6% lower which was attributed to non-linear material behaviour and the local buckling of the faces, although these were not quantified in experiments.

The increase in the stiffness of the joint as a result of the contact between the web and face plate resulted in a small increase in the post-buckling stiffness of the uncorroded sandwich plate. It indicates that the non-linearity of the joint must be considered for accurate response prediction in the case of thick plates with a small root gap. However, linear joint behaviour is justified for buckling analysis where the rotations at the T-joint are small. The importance of non-linearity of the joint for post-buckling response is reduced in corroded sandwich plates. There the face plates are so thin that the increase in D_{Qy} caused by the non-linearity of the joint is negligible. This is an extension to non-linear response from the work of Jelovica et al. [19], where the buckling strength of the sandwich plate with thin faces was unaffected by the joint stiffness.

The present study assumed that corrosion does not affect the laser welds. Aromaa et al. [6] showed that there are situations where crevice corrosion has very local affect on laser welds after two years of exposure. However, this is a localized phenomenon and the data on mechanical properties do not exist. In general, the mechanical properties of the T-joint will decrease and this could result in further deterioration of the buckling strength and post-buckling stiffness of the sandwich plate. However, this is just a hypothesis and requires experimental verification. Such experiments should also include longer exposure times, measurement of residual stresses and initial imperfections and the full-scale ultimate strength tests of the sandwich plates. As this study indicates, the instrumentation for such experiments should be carefully planned since it is expected that the failure happens at plate edges rather than at the mid-plane which is typical for isotropic plates.

6 Acknowledgments

The authors gratefully acknowledge the financial support of the Sustainable Breakthrough Innovations project, funded by the Finnish Metals and Engineering Competence Cluster (FIMECC), and the Graduate School of Engineering Mechanics, funded by the Finnish Academy of Sciences. Sincere thanks to Prof. J. N. Reddy for his valuable comments and improvement of the text. Sincere thanks also to Mr. Reijo Lindgren for his advice on modelling the connector-type element with Abaqus.

7 Appendix - Rotational stiffness of the T-joint of the sandwich plate

FE analysis of the T-joint is performed with Abaqus 6.9 to obtain the stiffness of the T-joint at larger rotation angles which might be expected as the sandwich plate enters the post-buckling response. The geometry of the T-joint resembles the measurements in Ref. [18]. The root gap between the web plate and face plate was measured to be below 10 μm. The weld is located at the centre of the web plate and has a thickness of 1.36 mm. The rotational stiffness of the T-joint was also experimentally established in the same publication.

The FE model (Fig. 10) is restrained by fixing the displacements of the nodes of the bottom surface of the face plate. The force is applied to the middle of the web plate, 22.6 mm from the interface of the web and face plate, as specified in Ref. [18]. The displacement of the web plate is measured in the middle of the plate, 24.2 mm from the same interface. The plane strain elements CPE4 and CPE3 are used.

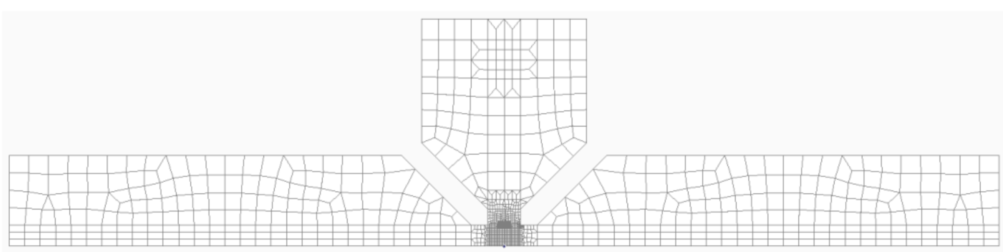

Fig. 10. *FE model used to simulate the rotational stiffness of the T-joint.*

The results of the FEM simulations on the rotational stiffness of the T-joint are presented in Fig. 11. The results are shown for a 50-mm-long specimen (the same as in the experimental study). It can be seen that the agreement with the experimental results is excellent for small displacements (Fig. 11a). This initial rotational stiffness is 107 kNm/m (calculated by dividing the moment by the resulting angle in the joint). The shape of the tip of the web plate was found to have a significant influence on the stiffness of the T-joint since it determines the contact area between the plates [18]. As the true shape of the tip is not known, the FE model is calibrated using this initial stiffness; see Fig. 12. A further increase in the displacements of the joint causes an increase in the stiffness as a result of the contact between the corner of the web plate and the face plate. The gap between the plates has an important role in determining when this contact occurs. Two root gaps are considered here: 2 μm and 10 μm, with the latter being the upper limiting value of the measurements in Ref. [18]. With these values, the resulting FEM curves bound the average experimental curve, as can be seen from Fig. 11. The secondary stiffness is twice as high as the initial stiffness. The force-displacement relation is transferred to the moment-angle relation, and it is used to define the behaviour of the connector element. The response using the connector element is quite in line with previously described results, as can be seen from Fig. 11(b).

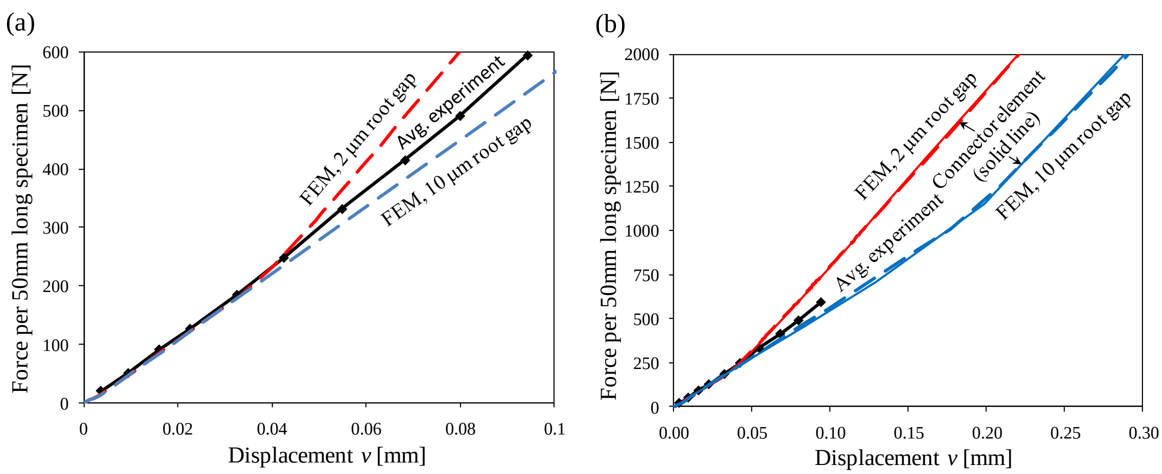

Fig. 11. *T-joint rotational stiffness (a) in the range of Ref. [18] and (b) at larger displacements.*

The ultimate load-carrying capacity of the T-joint is taken from the test results of Romanoff et al. [28]. The same test setup was used as described previously. The rotation angle of the joint was gradually increased and the force was measured, with the peak of the curve being defined as the ultimate force. The average ultimate force of 21 tests was 89 kN/m, which corresponds to an ultimate moment of 2011 Nm/m. The value is used in this study to check whether the joint failure occurs.

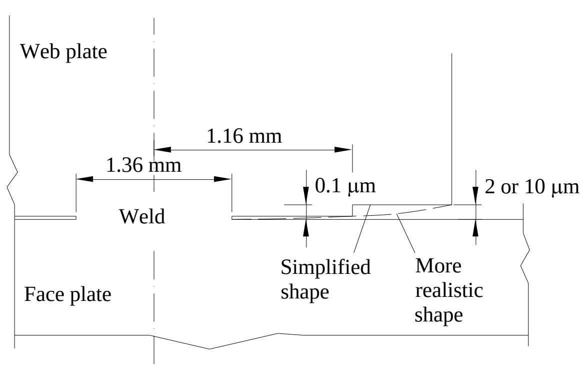

Fig. 12. *Shape of the T-joint.*

Jelovica, J., Romanoff, J. and Remes, H. "Influence of general corrosion on buckling strength of laser-welded web-core sandwich plates", Journal of Constructional Steel Research, Vol.101, 2014, p. 342-350.

8 References

[1] Rahgozar R. Remaining capacity assessment of corrosion damaged beams using minimum curves. Journal of Constructional Steel Research 2009; 65:299-307.

[2] Saad-Elden S, Garbatov Y, Guedes Soares C. Effect of corrosion severity on the ultimate strength of a steel box girder. Engineering Structures 2013; 49:560-71.

[3] SANDWICH Consortium. Synthesis report test results. TNO.ALL.Deliverable4.4-v1 03-03-03, 2003.

[4] Det Norske Veritas. Seawater exposure of laser-welded sandwich beams for evaluation of corrosion properties. Technical report No. 2003-1553, 2003.

[5] Jelovica J, Romanoff J, Ehlers S, Aromaa J. Ultimate strength of corroded web-core sandwich beams. Marine Structures 2013; 31:1-14.

[6] Aromaa J, Jelovica J, Forsen O. Corrosion of laser welded sandwich steel panels in seawater. Proc. EUROCORR, Istanbul, Turkey, 9-13.9.2012; pp. 1-11.

[7] Det Norske Veritas. Common structural rules for bulk carriers with length 90 meters and above. Høvik; 2008.

[8] Det Norske Veritas. Common structural rules for double hull oil tankers with length 150 meters and above. Høvik; 2008.

[9] Gardiner CP, Melchers RE. Corrosion analysis of bulk carriers, part 1: operational parameters influencing corrosion rates. Marine Structures 2003; 16:547–66.

[10] Tanker Structure Co-operative Forum. Condition evaluation and maintenance of tanker structures. London: Witherby; 1992.

[11] Det Norske Veritas. Projected guidelines for metal-composite laser-welded sandwich panels. 2004.

[12] Kolsters H, Zenkert D. Buckling of laser-welded sandwich panels: Part 1: elastic buckling parallel to the webs. Journal of Engineering for the Maritime Environment 2006; 220(2):67-79.

[13] Kolsters H, Zenkert D. Buckling of laser-welded sandwich panels: Part 2: elastic buckling normal to the webs. Journal of Engineering for the Maritime Environment 2006; 220(2):81-94.

[14] Kolsters H. Structural Design of Laser-Welded Sandwich Panels for Marine Applications. Doctoral Dissertation, Royal Institute of Technology, Department of Aeronautical and Vehicle Engineering, Stockholm 2004. Paper D: Buckling of laser-welded sandwich panels: Part 3: Ultimate strength and experiments.

[15] Taczala M, Banasiak W. Buckling of I-core sandwich panels. Journal of Theoretical and Applied Mechanics 2004; 42(2): 335-48.

[16] Kozak J. Problems of strength modeling of steel sandwich panels under in-plate loads. Polish Maritime Research 2006; S1:9-12.

[17] Jelovica J, Romanoff J. Load-carrying behaviour of web-core sandwich plates in compression. Submitted for review in Thin-Walled Structures.

[18] Romanoff J, Remes H, Socha G, Jutila M, Varsta P. The stiffness of laser stake welded T-joints in web-core sandwich structures. Thin-Walled Structures 2007; 45(4):453–62.

[19] Jelovica J, Romanoff J, Ehlers S, Varsta P. Influence of weld stiffness on buckling strength of laser-welded web-core sandwich plates. Journal of Constructional Steel Research 2012; 77:12-8.

[20] ABAQUS. 2012. User's manual, version 6.9.

[21] Romanoff J, Varsta P. Bending response of web-core sandwich plates. Composite Structures 2007; 81(2):292-302.

[22] Reddy JN. Mechanics of laminated composite plates and shells – Theory and analysis. 2nd ed. Boca Raton: CRC Press; 2000.

[23] Robinson JR. The buckling and bending of orthotropic sandwich panel with all edges simply-supported. The Aeronautical Quarterly 1955: 125-148.

[24] Melchers RE, Ahammed M, Jeffrey R, Simundic G. Statistical characterization of surfaces of corroded plates. Marine Structures 2010; 23:274-87.

[25] Romanoff J, Varsta P. Bending response of web-core sandwich beams. Composite structures 2006; 73:478-87.

[26] Kolsters H, Wennhage P. Optimisation of laser-welded sandwich panels with multiple design constraints. Marine Structures 2009; 22:154–71.

[27] Nordstrand T. Analysis and testing of corrugated board panels into the post-buckling regime, Composite Structures 2004; 63:189-99.

[28] Romanoff J, Remes H, Socha G, Jutila M. Stiffness and strength testing of laser stake welds in steel sandwich panels. Helsinki University of Technology, Ship Laboratory, Report M-291, Espoo; 2006.